RSC Advances

This article can be cited before page numbers have been issued, to do this please use: Y. Qiang, J. Jiang, Y. Xiong, H. Chen, J. Chen, S. Guan and J. Chen, *RSC Adv.*, 2016, DOI: 10.1039/C5RA27045F.

ROYAL SOCIETY OF CHEMISTRY

www.rsc.org/advances

RSC Advances

View Article Online
DOI: 10.1039/C5RA27045F

Paper

Facile synthesis of N/P co-doped carbons with tailored hierarchically porous structure for supercapacitor applications

Received 00th January 20xx,
Accepted 00th January 20xx

DOI: 10.1039/x0xx00000x

www.rsc.org/

Yiwei Qiang, Jingui Jiang, Yachao Xiong, Hao Chen, Jiayun Chen, Shiyou Guan* and Jianding Chen**

In this paper, nitrogen/phosphorous co-doped porous carbons (N/P-PCs) with hierarchical porosity were prepared by a one-step carbonization method, of which nitrogen-containing PAA/MMF is the precursor and phosphorous-containing sodium hypophosphite monohydrate is the novel pore-forming agent. The synergistic effect of multilevel porosity and heteroatomic functionalities results in good electrochemical performance. Tested as electrode materials for supercapactiors, N/P-PC-50 demonstrates a maximal specific capacitance of 177 F g^{-1} at a current density of 0.1 A g^{-1}, excellent rate capability (67% capacitance retention at 10 A g^{-1}) and superior cycling stability (no capacitance loss after 10000 cycles). In addition, N/P-PCs have the potential to be used for other applications, and this facile, low-cost and safe synthesis strategy provides a feasible route to develop many hierarchically porous carbon-based materials.

1. Introduction

As a new generation of energy storage devices, supercapacitors possessing fascinating electrochemical performance such as superior specific capacitance, excellent rate capability, high power density and outstanding cycling durability have attracted tremendous interest due to their role of bridging the gap between batteries and capacitors.[1-3] Carbonous materials are recognized as promising candidates of electrodes for supercapacitor applications, Li-ion batteries and fuel cells because of their easy availability, high electrical conductivity, environmental friendliness and good physicochemical stability.[4-7] Various carbon materials with different morphologies and compositions, such as graphene,[8,9] carbon nanotubes,[10,11] hierarchically porous carbons (e.g. carbide-derived carbons, activated carbons and templated carbons)[5,6,12] have been designed and studied. Among them, graphene, though possessing high conductivity and large specific surface area (over 2600 m^2 g^{-1}), has its limitation when utilized as electrode material due to its strong restacking tendency. For carbon nanotubes, high cost and purification difficulty are major hurdles that hinder their further practical applications.[13,14] In the past year, hierarchically porous carbons with a combination of macropores (>50nm), mesopores (2-50nm), micropores (<2nm) are extensively tested as supercapacitor electrode materials.[15-19] They have demonstrated excellent electrochemical performance when used as supercapacitor electrode materials due to the different roles of hierarchical pores: macropores allow ion-buffering and shorten the ion diffusion distance to interior surface, mesopores favour ion transport while micropores strengthen the electric-double-layer capacitance.[20,21] When compared with other carbon materials, hierarchically porous carbon electrodes can provide paths for efficient mass transport and ion penetrations,[22] making them to be considered as the ideal candidates for supercapacitor electrodes. Thus, it is urgent to develop novel hierarchically porous carbons for high-performance supercapacitors.

There are generally two ways in which carbons with high specific surface area (SSA) and multilevel porosity can be fabricated. One effective and typical method is physical (CO_2 or steam) or chemical (e.g. KOH, H_3PO_4, $ZnCl_2$)[23-25] activation. Another one is template-based approach adopts either hard-template (e.g. Silica or PS)[26,27] or soft template (e.g. Pluronic F127).[28] D. Saha et al.[29] synthesized mesoporous carbons from lignin with F127 as the soft template and the specific capacitance of obtained carbons was 77 F g^{-1}, which increased to 102.3 F g^{-1} after CO_2 activation. Both activation and templating methods involve complicated, time-consuming and low-yielding steps, adding to the process's overall cost and rendering them unsuitable for mass production.[30] It is especially true with hard-template method when costly templates are removed by expensive chemical etching using dangerous reagents. For this reason, it is still a great challenge and a pressing need to develop carbons with hierarchically porous structure by simple, eco-friendly and time-saving steps.

School of Materials Science and Engineering, East China University of Science and Technology, Shanghai 200237, P. R. China. Email: syguan@ecust.edu.cn (S. Guan), jiandingchen@ecust.edu.cn (J. Chen)

DOI: 10.1039/C5RA27045F

Scheme 1 Schematic illustration of the synthetic route and suggested morphology of N/P-PC-50

Along with porosity, the surface functionalities of carbon materials should be taken into consideration. It is widely recognized that heteroatoms (N, O, P), especially nitrogen can give rise to pseudocapacitance by Faradaic reactions as well as improve the wettability of carbon materials in electrolyte.[31-33] P-functionalities, on the other hand, are found to enhance specific capacitance, widen potential window and improve stability of carbon materials.[34, 35] However, plenty of nitrogen or phosphorous-doped carbon materials are obtained by post-treatment, such as treating with ammonia gas[36] or phosphoric acid,[37] which is tedious and harmful to the environment. Therefore, it is of great significance to develop carbon materials containing nitrogen/phosphorous functionalities without being post-treated.

In this work, we implement a green strategy to synthesize nitrogen/phosphorous co-doped hierarchically porous carbons through a single-step carbonization of nitrogen-doped precursors with phosphorous-containing pore-forming agent (Scheme 1). This novel strategy has the following advantages: (1) the precursors rapidly formed by sol-gel process result in high purity carbons with rich nitrogen functionalities, (2) the water-soluble sodium hypophosphite monohydrate plays two roles: as the pore-forming agent and as the phosphorous source, and (3) the preparation process is extremely facile involving no post-activation step. Therefore, carbons with hierarchically porous structure favourable for ion diffusion as well as nitrogen/phosphorous functionalities beneficial to enhancing electrical conductivity can be synthesized by this cost-effective method. The unique structure and heteroatom incorporation endow the obtained N/P-PC-50 with a specific capacitance of 177 F g^{-1} at a 0.1 A g^{-1}, a high rate capability (67% capacitance retention at 10 A g^{-1}) and a robust cycling stability (no capacitance loss after 10000 cycles). Besides, this safe and time-saving process of fabricating hierarchically porous carbons can be readily industrialized. We believe this strategy shows attractive prospects to prepare carbon-based materials for other practical applications, where abundant mesopores and macropores are highly favoured, such as catalysts or li-ion batteries.[38-40]

2. Experimental

2.1 Materials

Poly(acrylic acid) aqueous solution (PAA, Mn = 1800, PDI = 1.1, 52.0% solid) and methylated melamine-formaldehyde resin aqueous solution(MMF, Unibo HT580, 50.0% solid) were purchased from Shanghai Yiqian Co., Ltd. Pore forming agent-sodium hypophosphite monohydrate (98% solid) and HCl water solution (AR, 36.0~38.0% solid) were purchased from Sinopharm Chemical Reagent Co., Ltd. All reagents were used directly as received unless otherwise stated.

2.2 Fabrication of the carbons

The fabrication of the precursors is similar to our previous work.[41] The facile synthesis process of N/P-PC-50 can be described briefly as follows: 19.7g MMF containing 6.25g dissolved pore-forming agent were mixed up with 5.0g PAA, and kept at room temperature for 1 hour until the clear liquid converted to white solid as precursors. Then the precursors were placed in an oven cabinet dryer at 200℃ for 4 hrs, subsequently heated at 350℃ for 2hrs and finally 800℃ for 2hrs in a tubular furnace under N_2 atmosphere with a heating rate of 3℃ min^{-1}. Then the samples were washed with HCl water solution and distilled water until the filtrate was neutral. Finally the sample was dried at 80℃ for 12 hrs. The final carbons were named after N/P-PC-X. N/P-PC stands for nitrogen/phosphorous co-doped porous carbons and X means the weight ratio of pore-forming agent to PAA/MMF. In addition, the nitrogen-doped porous carbons synthesized by precursors without pore-forming agent were simply named as NPC.

2.3 Sample Characterization

Scanning electron microscopy (SEM) measurement was conducted on S-3400 (Hitachi, Japan) to observe the morphology of prepared carbons. Transmission electron microscopy (TEM) images were obtained on JEM-2100 (JEOL, Japan) equipped with a Genesis XM2 energy dispersive spectrum (EDS) analysing system. Raman spectra were performed on an InVia Raman microscope (Renishaw, UK) with 514.5 nm diode laser excitation. Powder X-ray diffraction (XRD) patterns were recorded on a D/MAX 2550VB/PC diffractometer (Rigaku, Japan) using Cu-Kα radiation (λ=0.154nm). The porosity of carbons were identified using nitrogen adsorption-desorption isotherms on an ASAP 2010 instrument (Micromeritics, USA) at 77 K. Brunaer-Emmett-Teller (BET) and Barrett-Joyner-Halendar (BJH) methods were adopted to obtain the specific surface area and calculate the pore size distribution, respectively. X-ray photoelectron spectroscopy (XPS) analysis was carried out via an ESCALAB 250Xi spectrometer (Thermo Fisher, USA) with Al Kα radiation (hv= 1486.6 eV) in order to determine the nitrogen/phosphorous functional groups present on the surface of all carbons. The binding energy scale was regulated by setting C1s transition at 284.6 eV.

2.4 Electrochemical measurements

For electrochemical measurements, the working electrode was prepared by mixing 80wt% active materials with 10wt% polytetrafluoroethylene (PTFE) as a binder and 10wt% acetylene back carbon (AB) powder as the conductive assistant and pressing the blend onto titanium mesh under a pressure of 10MPa. Each working electrode weighing 5mg contained 4mg active materials and was dipped in 1M H_2SO_4 for 24hrs. Then the electrochemical measurements were operated on an electrochemical analyzer CHI 660D (Shanghai Chenhua Co., Ltd, China) using a three-electrode system in aqueous solution. Ag/AgCl electrode (3M KCl solution) and platinum plate were used as the reference and counter

electrode, respectively. The cyclic voltammetry (CV) and galvanostatic charge/discharge (CD) measurements were carried out in a potential window from –0.1 to 0.9 V. Electrochemical impedance spectroscopy (EIS) were performed in the frequency range from 100 kHz to 0.01 Hz with an AC amplitude of 10 mV.

The specific capacitances of all carbons are calculated from the slopes of the discharge curves by the following equation:

$$C = \frac{I \times \Delta t}{m \times \Delta U}$$

In this equation, C (F g^{-1}) is the specific capacitance value of the active materials, I (A) is the constant discharging current, Δt (s) is the discharging time, m(g) is the mass of the active materials within the working electrode and ΔU is the discharging potential window (1.0 V).

3. Results and discussions

3.1 Morphology and structure

The SEM images of the N/P-PCs (Fig.1 a-d) clearly demonstrate that hierarchically porous texture of N/P-PCs can be developed by increasing the weight ratio of pore-forming agent to PAA/MMF. It can be seen that NPC prepared with no pore-forming agent exhibits a smooth surface with only a few macropores. Compared to NPC, N/P-PC-20 possesses a rougher surface with more macropores. N/P-PC-50, however, shows a very different beehive-like morphology constituted by a large number macropores ranging from about 50nm to 2μm in diameter, which were mainly generated by pyrolysis of precursors and removal of the pore-forming agent in precursors. Fig. 2b-d show typical TEM images of N/P-PC-50 which is composed of partially overlapped graphitic layers and highly disordered pore structure. They further reveal that compared with N/P-PC-20 (Fig. 2a) with only a few pores, N/P-PC-50 develop a different texture containing abundant macropores (around 300nm) and large mesopores (20-50nm). Unlike conventional materials with high surface area primarily contributed by micropores, N/P-PC-50 possesses plenty of mesopores and macropores that are more accessible for electrolyte ions and are capable of reducing ion-transport resistance significantly.

Fig. 1 SEM images of (a) NPC, (b) N/P-PC-20 and (c-d) N/P-PC-50 at different magnifications

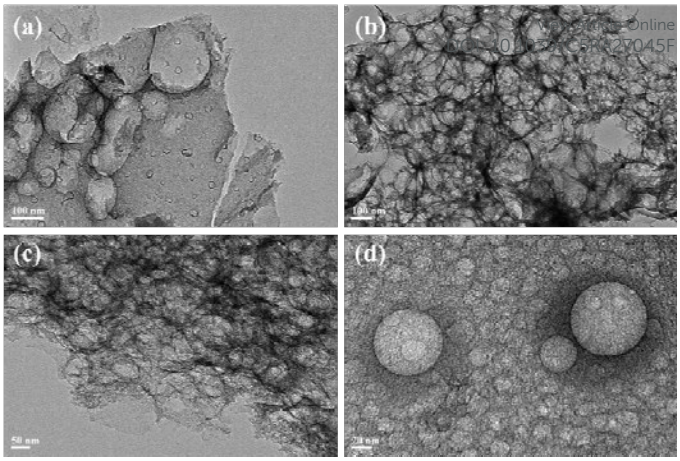

Fig. 2 TEM images of (a) N/P-PC-20 and (b-d) N/P-PC-50 at different magnifications

As shown in Fig. 3, RAMAN, XRD and BET measurements were employed to further understand the porosity and structure of N/P-PCs. Raman spectra (Fig. 3a) of the N/P-PCs displays two obvious peaks around 1350 cm^{-1} and 1580 cm^{-1}, representing disorder-associated D bands and graphite-related G bands typical of carbon materials, respectively.[4, 42] With the increase of proportion of pore-forming agent in precursors, it is obvious that the intensity of D bands increases as well, indicating a less ordered crystalline structure. As represented in Fig. 3b, wide-angle XRD patterns of N/P-PCs display one strong diffraction peak at around 23° and another weak diffraction peak at around 43° assigned to the (002) and (100) planes, respectively.[43] It can been seen that the intensity of these two peaks decreases from NPC to N/P-PC-50, indicating that the crystalline structures of N/P-PCs are destructed by pore-forming agent, which is in good accordance with Raman spectra.

Fig. 3c-d depict the N_2 adsorption–desorption isotherms and the pore size distribution (PSD) curves recorded from adsorption isotherms and calculated by Barrett–Joyner–Halendar (BJH) method. The type Ⅱ sorption isotherm of NPC indicates the nonexistence of porosity which is also confirmed by PSD. In comparison, the volume

Fig. 3 (a) Raman spectra, (b) Wide-angle XRD patterns under N_2, (c) Nitrogen adsorption–desorption isotherms, (d) pore size distribution curves of NPC and N/P-PCs

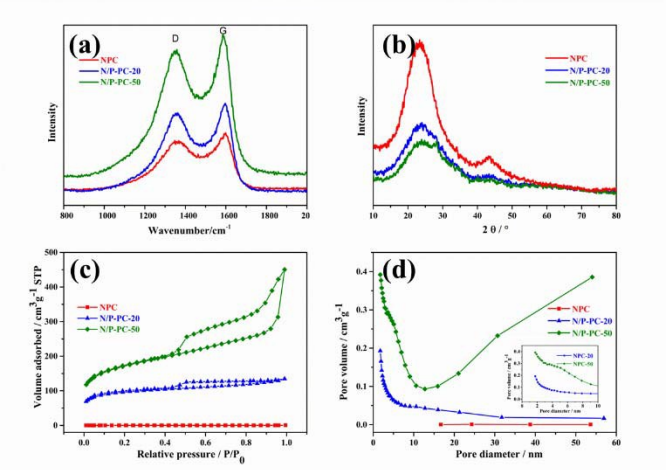

View Article Online
DOI: 10.1039/C5RA27045E

Fig. 4 (a) XPS survey spectrum of N/P-PC-50 and its corresponding (b) N1s and (c) P2p spectrum

adsorbed of N/P-PC-20 and N/P-PC-50 increases dramatically, implying a further developed porous structure. N/P-PC-50 displays a type Ⅳ sorption isotherm with a clear hysteresis loop in the relative pressure (P/P_0) range of 0.4-1.0, showing a presence of mesopores. In addition, the obvious steep peak at a high relative pressure (P/P_0>0.9) proves the existence of a large number of macropores in N/P-PC-50.[33, 41] The pore size distribution verify that both N/P-PC-20 and N/P-PC-50 have micropores along with plenty mesopores which have a narrow size distribution in the range of 2-6nm. Noticeably, the pore volume of N/P-PC-50 increases when diameter increases from 20nm, indicating the existence of large mesopores and macropores. We assume that this is a result of a larger proportion of pore-forming agent in precursors and the creation of large pores due to the collapse of small ones during carbonization. The BET surface area and total pore volume of the obtained porous carbons are summarized in Table 1. Compared to NPC which possesses negligible porosity with a tiny BET specific surface area and zero pore volume, the N/P-PCs demonstrated better-developed porosity. The BET specific surface area and pore volume increase from 302.2 $m^2 g^{-1}$ and 0.10 $cm^3 g^{-1}$ for N/P-PC-20 to 571.2 $m^2 g^{-1}$ and 0.55 $cm^3 g^{-1}$ for N/P-PC-50, respectively, which imply the important role of pore-forming agent in tuning porosity development. Though the surface are of N/P-PC-50 is lower than many reported porous carbons due to limited micropores, it is still higher than that of some reported literatures, such as P/N co-doped microporous carbons (surface area of 353 $m^2 g^{-1}$)[34] or porous carbon from co-polymer of PAN and PBA without any activation (surface area 500 $m^2 g^{-1}$). [44] In addition, many researchers discover that there is no linear relationship between the surface area and the specific capacitance. They point out that only the surface accessible to ions can contribute to efficient energy storage.[7, 45]

Table 1 Porous property identified from BET and BJH, elemental composition from XPS spectrum of NPC, N/P-PC-20 and N/P-PC-50

Sample	S_{BET} ($m^2 g^{-1}$)			Pore volume ($cm^3 g^{-1}$)	Elemental Composition (XPS) [%]	
	Total	Micro	External		N	P
NPC	0.2	0.9	-	0.00	5.1	0
N/P-PC-20	302.2	160.5	141.7	0.10	7.4	2.2
N/P-PC-50	571.2	189.8	381.5	0.55	6.5	3.3

XPS analysis was conducted to identify the heteroatom content and the chemical state of nitrogen and phosphorous species of synthesized carbons. The XPS survey spectrum (Fig. 4a) displays that N/P-PC-50 consists of 6.5% nitrogen and 3.3% phosphorous. The three peaks of N1s spectrum (Fig. 4b) correspond to pyridinic nitrogen (398.7eV), pyrrolic nitrogen (400.1eV) and graphitic nitrogen (401.1eV), respectively. It has been widely accepted that besides improving the wettability of the electrode, pyridinic and pyrrolic nitrogen can generate pseudocapacitance through redox reactions. In addition, when distributed in ion-accessible pores, graphitic nitrogen are found to facilitate the transportation of electrons and enhance the specific capacitance.[34,37,43,46] For phosphorous, the peak at 133.3 eV (Fig. 4c) can be ascribed to phosphate and/or pyrophosphate groups formed by the decomposition of pore-forming agent. As listed in Table 1, the nitrogen content of the obtained carbons is around 6% while the content of phosphorous increases from 0 for NPC to 2.2% for N/P-PC-20 and 3.3% for N/P-PC-50, indicating that the ratio of pore-forming agent to PAA/MMF can be used not only to tune the porosity development but also to tailor the amount of phosphorous functionalities. EDX spectrum (Fig. 5d) confirms the presence of phosphorous heteroatom in the carbon matrix. The strong signal of Cu in EDX spectrum is derived from the TEM copper grids and the missing of nitrogen signal is due to the limited ability of the EDS analysing system to detect light elements. EDX mapping (Fig. 5b-c) was performed to investigate the element distribution of N/P-PC-50. Results indicate that C and P elements are distributed in the whole sample homogenously.

3.2 Electrochemical performance

The unique structure of N/P-PCs inspired us to investigate their

Fig. 5 (a) TEM image of N/P-PC-50 and the corresponding elemental mappings of (b) C, (c) P and (d) EDX spectrum.

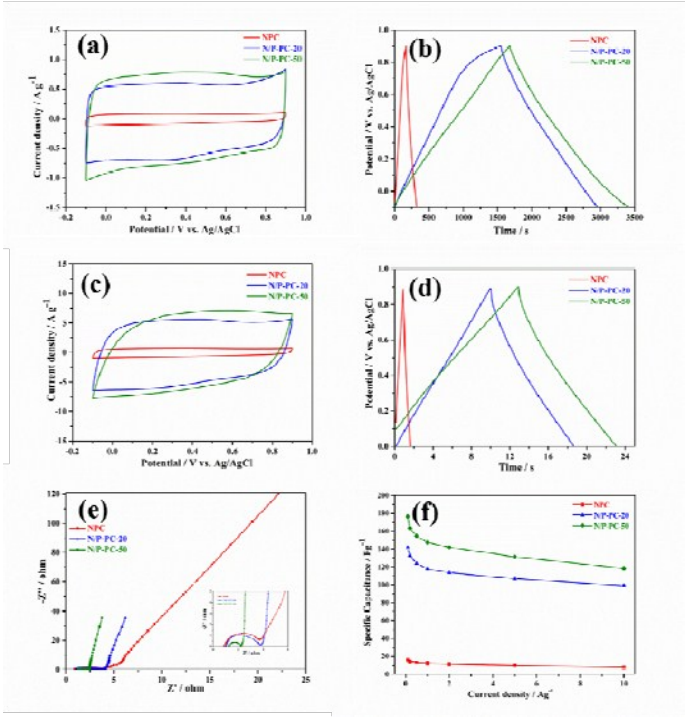

Fig. 6 (a) CV curves of carbons at a scan rate of 5 mV s^{-1}, (b) Galvanostatic charge/disharge curves of carbons at a current density of 0.1 A g^{-1}, (c) CV curves of carbons at a scan rate of 50 mV s^{-1}, (d) Galvanostatic charge/discharge curves of carbons at a current density of 10 A g^{-1}, (e) Nyquist plots of carbons, (f) The specific capacitance as a function of current density (0.1-10 A g^{-1})

electrochemical performance as electrode materials for supercapacitors. Cyclic voltammetry (CV), galvanostatic charge-discharge and electrochemical impedance spectroscopy (EIS) were measured in a 1M H_2SO_4 aqueous electrolyte by a three-electrode system. As shown in Fig. 6a, the CV curve at a scan rate of 5 mV s^{-1} of N/P-PC-50 exhibits an almost rectangular and symmetric shape with slight distortions which indicates typical electric double-layer capacitance (EDLC) behaviour while reversible humps from line demonstrate pseudocapacitance offered by the nitrogen-containing functional groups in MMF and phosphorous functionalities in pore-forming agent. It can be noticed that the rectangular shape of N/P-PC-50 is maintained relatively better than other carbons at either low (Fig. 6a) or high scan rate (Fig. 6c), indicating lower resistance of ion diffusion and more rapid forming of double layer. Fig. 6b and Fig. 6d show the galvanostatic charge-discharge profiles of all carbons at a current density of 0.1 A g^{-1} and 10 A g^{-1}, respectively. It can be seen that the discharging time and corresponding charging time is almost equal and that all curves show a linear and symmetric shape, revealing an ideal electric double layer capacitive behaviour which is consistent with CV results. It can also be seen that the curve of N/P-NC-20 is slightly distorted and the charging time is longer than the discharging time at a current density of 0.1 A g^{-1}. This can be ascribed to the relatively larger transport resistance of N/P-PC-20 compared to N/P-PC-50, leading to a more difficult charging process.

N/P-PC-20, compared with NPC with a low specific capacitance (15.7 F g^{-1}), displays a much longer discharging time and its capacitance is 142 F g^{-1}. N/P-PC- 50 exhibits a capacitance of 177 F

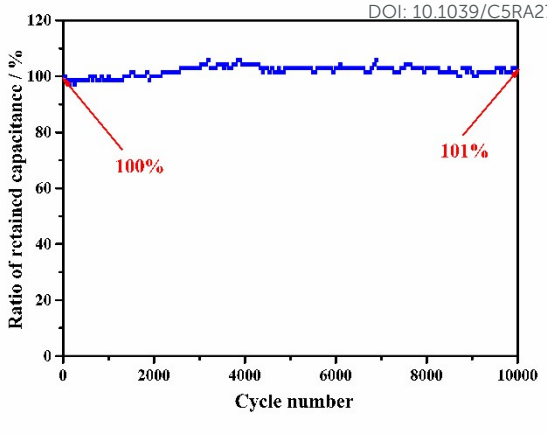

Fig. 7 Cycling stability of N/P-PC-50 at a current density of 2 A g^{-1}

g^{-1}, which is almost 11 times of that of NPC, due to a well-developed hierarchically porous structure and the co-doping of nitrogen and phosphorous functionalities. This is further confirmed by the EIS measurements of all carbons (Fig 6e). In comparison with NPC and N/P-PC-20, N/P-PC-50 shows the smallest semicircle at high frequency indicating lowest charge transfer resistance and most vertical line at low frequency representing lowest diffusion resistance. In addition, the specific capacitance as a function of current density of all carbons (Fig. 6f) shows that the N/P-PC-50 possesses a good rate capability of 67% capacitance retention when the current density increases by 100 times (from 0.1 A g^{-1} to 10 A g^{-1}). Furthermore, the long-term cycling stability is another significant parameter for supercapacitors.[47] As shown in Fig. 7, N/P-PC-50 shows excellent cycling stability with no capacity decrease over 10000 cycles. The slight increase (ca.1%) of the specific capacitance after 10000 cycles is probably due to the continuously activation of the electrode materials during the charge-discharge process.[48]

The above electrochemical results clearly demonstrate that N/P-PC-50 possesses excellent electrochemical performance. Although its specific capacitance (177 F g^{-1} at a current density of 0.1 A g^{-1}) is lower than those of many templated or activated porous carbons (200-300 F g^{-1}), it is still superior to some recently reported nitrogen-doped carbons based on aqueous electrolyte, such as lignin-derived hierarchical porous carbons (160 F g^{-1} at 0.1 A g^{-1}),[17] activated lignin-derived mesoporous carbons (102.3 F g^{-1} at 0.1 A g^{-1}),[29] P/N co-doped microporous carbons (154 F g^{-1} at 0.1 A g^{-1}),[34] co-polymer templated nitrogen-enriched porous carbons (166 F g-1 at 0.1 A g^{-1})[44] and nitrogen-doped carbon-coated graphene (170 F g^{-1} at 0.1 A g^{-1}).[49] Considering the extremely facile and time-saving fabrication method, N/P-PC-50 is a promising electrode material for supercapacitors and has the potential for industrial applications. Post-activation such as KOH activation of N/P-PC-50 can be further employed if larger specific supercapacitance is intended.

4. Conclusions

In summary, nitrogen/phosphorous co-doped carbons with hierarchically porous structure were simply prepared by pyrolysis of precursors formed by sol-gel process. Sodium hypophosphite

monohydrate not only functions as a novel pore-forming agent but also induces phosphorous into carbon. N/P-PC-50 demonstrates greatly enhanced electrochemical performance in 1M H_2SO_4 compared to NPC, including specific capacitance of 177 F g^{-1}, excellent rate capability (67% capacitance retention at 10 A g^{-1}) and outstanding cycling stability(no capacitance decay after 10000 cycles). Its excellent energy storage performance benefits from: (1) abundant macropores as the ion-buffering reservoirs and mesopores as the ion transport pathways help for the fast transport and diffusion of ions into micropores, (2) micropores increase the interfacial area between electrolyte and electrode and serve as ion traps for efficient energy storage, [5, 50] and (3) the existence of N and P heteroatomic functionalities in N/P-PC-50 generates pseudocapacitance, improves the wettability of the porous carbon and thus enhances electrochemical performance. Besides, we believe such a hierarchical structure with abundant macropores and mesopores would have great potential for other functional applications apart from supercapacitors, such as catalyst support, gas storage and Li- and Na-ion batteries.

Acknowledgements

The authors are grateful for the financial support from National Natural Science Foundation of China (No. 21274043).

References

1 R. Kötz, M. Carlen, *Electrochim. Acta*, 2000, **45**, 2483-2498.
2 M. Winter and R.J. Brodd, *Chem. Rev.*, 2004, **104**, 4245-4270.
3 J. Jeon, L. Zhang, J. L. Lutkenhaus, D. D. Laskar, J. P. Lemmon, D. Choi, M. I. Nandasiri, A. Hashmi, J. Xu, R. K. Motkuri, C. A. Fernandez, J. Liu, M.P. Tucker, P. B. McGrail, B. Yang and S. K. Nune, *ChemSusChem*, 2015, **8**, 428-432.
4 S. Wang, J. Zhang, P. Shang, Y. Li, Z. Chen and Q. Xu, *Chem. Commun.*, 2014, **50**, 12091-12094.
5 L. Qie, W. Chen, H. Xu, X. Xiong, Y. Jiang, F. Zhou, X. Hu, Y. Xin, Z. Zhang and Y. Huang, *Energy Environ. Sci.*, 2013, **6**, 2497-2504.
6 J. Liang, S. Chen, M. Xie, Y. Wang, X. Guo, X. Guo and W. Ding, *J. Mater. Chem. A*, 2014, **2**, 16884-16891.
7 L. Dai, D. W. Chang, J. Baek and W. Lu, Small, 2012, **8**, 1130-1166.
8 H. Chang and H. Wu, *Energy Environ. Sci.*, 2013, **6**, 3483-3507.
9 Y. Yoon, K. Lee, S. Kwon, S. Seo, H. Yoo, S. Kim, Y. Shin, Y. Park, D. Kim, J. Choi and H. Lee, *ACS Nano*, 2014, **8**, 4580-4590.
10 H. Liu, H. Song, X. Chen, S. Zhang, J. Zhou, Z. Ma, *J. Power Sources*, 2015, **285**, 303-309
11 V. Kuzmenko, O. Naboka, M. Haque, H. Staaf, G. Goransson, P. Gatenholm and P. Enoksson, *Energy*, 2015, **90**, 1490-1496
12 P. Gao, W. Tsai, B. Daffos, P. Taberna, C. Pérez, Y. Gogotsi, P. Simon, F. Favier, *Nano Energy*, 2015, **12**, 197–206.
13 H. Jiang, P. Lee and C. Li, *Energy Environ. Sci.*, 2013, **6**, 41–53.
14 C. Liu, Z. Yu, D. Neff, A. Zhamu and B. Jang, *Nano Lett.*, 2010, **10**, 4863–4868
15 S. Song, F. Ma, G. Wu, D. Ma, W. Geng and J. Wan, *J. Mater. Chem. A*, 2015, **3**, 18154–18162
16 C. Longa, X. Chen, L. Jiang, L. Zhi, Z. Fan, *Nano Energy*, 2015, **12**, 141–151.
17 W. Zhang, H. Lin, Z. Lin, J. Yin, H. Lu, D. Liu and M. Zhao, *ChemSuschem*, 2015, **8**, 2114-2122.
18 C. Wang, M. O'Connell and C. Chan, *ACS Appl. Mater. Interfaces*, 2015, **7**, 8952-8960.
19 Y. Li, C. Lu, S. Zhang, F. Su, W. Shen, P. Zhou and C. Mae, *J. Mater. Chem. A*, 2015, **3**, 14817–14825
20 D. Wang, F. Li, M. Liu，G. Lu and H. Cheng, *Angew. Chem. Int. Ed.*, 2007, **120**, 379-382.
21 H. Liu, J. Wang, C. Wang and Y. Xia, *Adv. Energy Mater.*, 2011, **1**, 1101-1108.
22 S. Chaudhari, S. Kown and J. Yu, *RSC Adv.*, 2014, **4**, 38931-38938.
23 Y. Zhu, S. Murali, M. D. Stoller, K. J. Ganesh, W. Cai, P. J. Ferreira, A. Pirkle, R. M. Wallace, K. A. Cychosz, M. Thommes, D. Su, E. A. Stach and R. S. Ruoff, *Science*, 2011, **24**, 1537-1541.
24 F. Wang, S. Xiao, Y. Hou, C. Hu, L. Liu and Y. Wu, *RSC Adv.*, 2013, **3**, 13059-13084.
25 Y. Huang, S. Hu, S. Zuo, Z. Xu, C. Han and J. Shen, *J. Mater. Chem.*, 2009, **19**, 7759-7764.
26 H. Nishihara and T. Kyotani, *Adv. Mater.*, **24**, 4473-4498.
27 S. H. Choi and Y. C. Kang, *ChemSusChem*, 2015, **8**, 2260-2267.
28 C. Huang, Q. Zhang, T. Chou, C. Chen, D. Su and R. Doong, *ChemSusChem*, 2012, **5**, 563-571.
29 D. Saha,Y. Li, Z. Bi, J. Chen, J. K. Keum, D. K. Hensley, H. A. Grappe, H. M. Meyer, S. Dai, M. P. Paranthaman and A. K. Naskar, *Langmuir*, 2014, **30**, 900-910.
30 P. Dhanya, V. Aravindan, S. Madhavi and S. Ogale, *Energy Environ. Sci.*, 013, **7**, 728-735.
31C. O. Ania, V. Khomenko, E.R. Piñero, J. B. Parra and F. Béguin, *Adv. Fun. Mater.*, 2007, **17**, 1828-1836.
32 Y. Zhai, Y. Dou, D. Zhao, P. F. Fulvio, R. T. Mayes and S. Dai, *Adv. Mater.*, 2011, **23**, 4828-4850.
33 G. Ma, F. Ran, H. Peng, K. Sun, Z. Zhang, Q. Yang and Z. Lei, *RSC Adv.*, 2015, **5**, 83129-83138.
34 C. Wang, L. Sun, Y. Zhou, P. Wan, X. Zhang, J. Qiu, *Carbon*, 2013, **59**, 537-546.
35 H. Denisa, A. M. Puziy, O. I. Poddubnaya, S. Fabian, J Tascón, G. Lu, *J. Am. Chem. Soc.*, 2009, **131**, 5026–5027.
36 V. Bairia, U. Nasinia, S. Ramasahayama, S. Bourdob, T. Viswanathan, *Electrochim. Acta*, 2015, **182**, 987-994.
37 X. Sun, P. Cheng, H. Wang, H. Xu, L. Dang, Z. Liu, Z. Lei, *Carbon*, 2015, **92**, 1-10.
38 C. Parlett, K. Wilson and A. Lee, *Chem. Soc. Rev.*, 2013, **42**, 3876-3893.
39 Z. Guo, D. Zhou, X. Dong, Z. Qiu, Y. Wang and Y. Xia, *Adv. Mater.*, 2013, **25**, 5668-5672.
40 A. Vu, Y. Qian and A. Stein, *Adv. Energy Mater.*, 2012, **2**, 1056-1085.
41 J. Jiang, L. Bao, Y. Qiang, Y. Xiong, J. Chen, S. Guan, J. Chen, *Electrochim. Acta*, 2015, **158**, 229-236.
42 J. Chen, Y. Liu, W. Li, H. Yang and L. Xu, *RSC Adv.*, 2015, 5, **9**, 98177-98183.
43 C. Wang, Y. Zhou, L. Sun, P. Wang, X. Zhang, J. Qiu, *J. Power Sources*, 2013, **239**, 81–88.
44 M. Zhong, E. Kim, J. McGann, S. Chun, J. Whitacre, M. Jaroniec, K. Matyjaszewski and T. Kowalewski, *J. Am. Chem. Soc.*, 2012, **134**, 14846–14857.
45 T. Gao, W. Xu, L. Gong, Z. Wang, Z. Yang, Y. Song and Y. Xiong, *RSC Adv.*, 2015, **5**, 33767-33.
46 U. Nasini, V. Bairi, S. Ramasahayama, S. Bourdo, T. Viswanathan, A. Shaikh, *J. Power Sources*, 2014, **250**, 257-265.
47 F. Ran, X. Zhang, Y. Liu, K. Shen, X. Niu, Y. Tan, L. Kong, L. Kang, C. Xu and S. Chen, *RSC Adv.*, 2015, **5**, 87077-87083.
48 X. Lu, D. Zheng, T. Zhai, Z. Liu, Y. Huang, S, Xie and Y. Tong, *Energy Environ. Sci.*, 2011, **4**, 2915-2921.

49 K. Kim and S. Park, *Electrochimi. Acta*, 2011, **56**, 6547-6553.
50 T. Yang, R. Zhou, D. Wang, S. P. Jiang, Y. Yamauchi, S. Z. Qiao, M. J. Monteiro and J. Liu, *Chem. Commun.*, 2015, **51**, 2518-2521.

View Article Online
DOI: 10.1039/C5RA27045F

View Article Online
DOI: 10.1039/C5RA27045F

A facile process was designed to synthesize nitrogen/phosphorous co-doped hierarchically porous carbons with excellent performance for supercapacitors.